ISSN 1062-7391, Journal of Mining Science, 2019, Vol. 55, No. 1, pp. 157–168. © Pleiades Publishing, Ltd., 2019.
Russian Text © The Author(s), 2019, published in Fiziko-Tekhnicheskie Problemy Razrabotki Poleznykh Iskopaemykh, 2019, No. 1, pp. 172–184.

MINING
THERMOPHYSICS

Adjustment of Thermophysical Rock Mass Properties in Modeling Frozen Wall Formation in Mine Shafts under Construction

L. Yu. Levin*, M. A. Semin, and A. V. Zaitsev

Mining Institute, Ural Branch, Russian Academy of Sciences, Perm, 614007 Russia
**e-mail: aerolog_lev@mail.ru*

Received January 18, 2018
Revised January 23, 2019
Accepted January 29, 2019

Abstract—Modeling of heat exchange processes in water-saturated rock mass during shafting with artificial freezing is performed. The problem of adjusting thermophysical properties of rock layers by the experimental measurements of temperature in the check thermal wells spaced from the freezing perimeter is analyzed. In terms of the abuilding shafts at Nezhinsky Mining and Processing Plant, significance of adjusting the the thermophysial parameters borrowed from the geological engineering survey data is illustrated. The number of independent adjustment parameters is determined from the analysis of the system of equations in two-dimensional two-phase Stefan problem in the dimensionless form. An inverse Stefan problem is formulated for a horizontal layer of rocks. The numerical algorithm is proposed for the inverse Stefan problem solution based on the gradient descent method. The algorithm minimizes functional of discrepancies between the model and measurement temperatures at the locations of the check wells. The functional of discrepancies in the phase space of the thermophysical properties and the algorithm convergence are analyzed.

Keywords: Frozen wall, inverse Stefan problem, model parameter adjustment, gradient descent method, finite difference method, mine shaft.

DOI: 10.1134/S1062739119015419

INTRODUCTION

Implementation of complex process systems in any industry and, in particular, mining is not complete without prior mathematical modeling of related physical and engineering processes, forecasting of system parameters in the future. This is done to minimize material costs and risks of accidents.

In this paper, heat exchange processes are simulated mathematically in water-saturated rock mass during shafting by artificial freezing of rocks [1]. When applying this method, wells are drilled along the contour of shaft designed for sinking, into which freezing pipes are lowered. Due to the operation of freezing stations, a cooling agent (brine) is circulated through the pipes. As a result of cooling brine circulation in the freezing pipe, the surrounding rock mass is gradually cooled, and the water containing in the rock mass crystallizes. After some time, single ice cylinders are formed around the freezing pipes, which subsequently close in to form a frozen wall. The latter serves to prevent the groundwater penetration to the opening of abuilding shaft during the entire construction process, up to the building of tubing columns and sealing of their joints (Fig. 1).

Shafting with artificial freezing of rocks requires systematic monitoring of their condition [2]. There are a number of control methods, the most advanced of them is continuous monitoring of the rock mass temperature using check thermal wells located at some distance from the contour of freezing pipes (Fig. 1) [3].

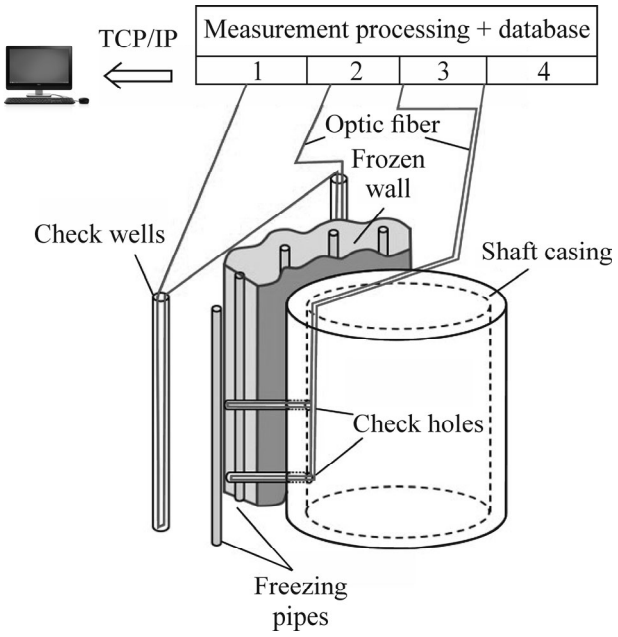

Fig. 1. The system of rock mass artificial freezing near abuilding shaft, the system for monitoring frozen wall condition.

Before shaft construction starts, engineering and geological surveys are carried out on the industrial site: investigations of physico-mechanical, thermophysical, mineralogical and petrographic properties of rock samples taken from wells. Thermophysical parameters of rock layers obtained as a result of engineering and geological surveys often have high inaccuracy, and mathematical models describing heat and mass exchange processes in rocks and constructed using these parameters are ineffective in solving practical problems.

The results of the data analysis on rock mass freezing obtained in monitoring of the temperature near abuilding shafts nos. 1–2 at the Nezhin Mining and Processing Plant (GOK) show a significant difference between the initial values of thermal parameters taken from engineering geological surveys and their adjusted values on the measured temperatures of rocks in check thermal wells. Figure 2 presents a comparative analysis of discrepancies between the initial and adjusted properties of different rock layers in terms of dimensionless thermophysical complexes (Fourier numbers Fo and Stefan numbers Ste) determined by the formulas:

$$\mathrm{Fo}_i = \frac{\lambda_i t_\Sigma}{\rho_i c_i l^2}, \quad \mathrm{Ste}_i = \frac{c_i (T_0 - T_F)}{wL}, \tag{1}$$

where ρ is the rock mass density, kg/m^3; c is the rock mass heat capacity, J/(°C·kg); λ is the rock mass thermal conductivity, W/(°C·m); w is the moisture content in the rock mass, kg/kg; L is specific heat capacity of the phase transition, J/kg; T_0 is the temperature of undisturbed rock mass, °C; T_F is the freezing temperature, °C; t_Σ is characteristic time (modeling time), c; l is characteristic dimension of computational domain, m.

From Fig. 2 it is evident that relative discrepancy reaches 70%. It was difficult to reliably determine the relative discrepancy of individual physical properties, since the temperature field depends on the combination of thermophysical properties in (1).

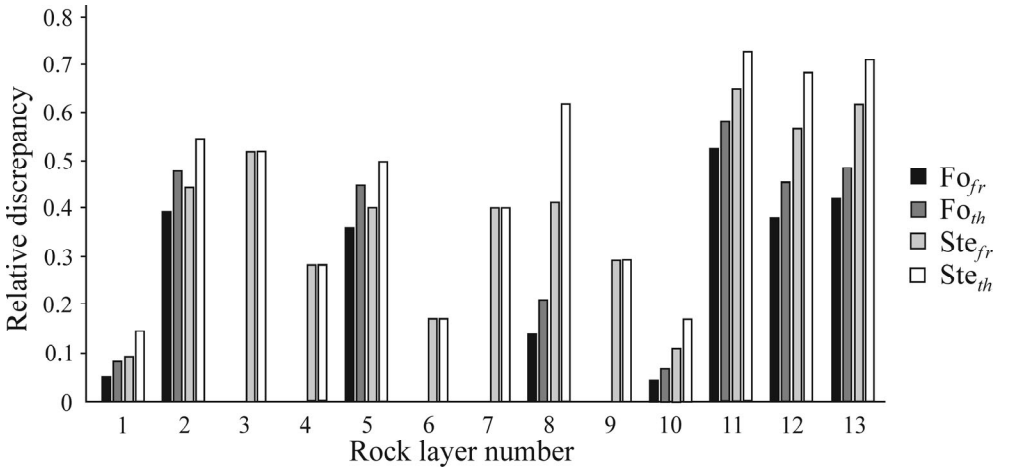

Fig. 2. Relative discrepancies of thermophysical properties of rock layers for the conditions of industrial site of Nezhinsky GOK mine: Fo$_{fr}$, Ste$_{fr}$—Fourier and Stefan numbers for frozen rock mass; Fo$_{th}$, Ste$_{th}$—Fourier and Stefan numbers for thawed rock mass.

Adjustment was made by minimizing the temperature discrepancy criterion I at check wells measured experimentally and calculated theoretically by solving direct Stefan problem:

$$I = \sum_{i=1}^{N_c} \int_0^{t_\Sigma} (T_i^{(e)} - T_i^{(m)}) dt \,. \tag{2}$$

Here, $T_i^{(m)}$ and $T_i^{(e)}$ are the model and experimental temperatures at an i-th well, °C; N_c is the number of check wells; t_Σ is the freezing time, days. The formulation of direct Stefan problem used in [3] will be considered further.

The modeling results of frozen wall formation dynamics obtained from the initial engineering-geological and adjusted values differ significantly from each other. This indicates the need for adjustment of thermophysical parameters of rock layers obtained from engineering-geological surveys, before using them to predict the formation time for frozen wall of the required thickness and determine the energy-efficient operating modes of the freezing stations.

The issue of thermophysical rock properties adjustment applicably to the problem of controlling frozen wall formation has not previously been considered. The available works on frozen wall are either dedicated to solving the direct Stefan problem using the preset thermophysical rock properties, which are accepted as true [4–8], or contain a description of experimental studies on frozen wall condition and shaft sinking technology [1, 5, 9, 10].

This paper is dedicated to the selection of adjustment parameters from a variety of thermophysical properties of rock layers and construction of an automated method for adjusting thermophysical properties, based on solving coefficient inverse Stefan problem.

1. SELECTION OF ADJUSTMENT PARAMETERS

The adjustment parameters are thermophysical properties of the rock layers—heat capacity, thermal conductivity, density, moisture content. An increased inaccuracy of their determination in the course of engineering and geological surveys is caused by the following factors [11]:

1. Insufficiency of core sampling and insufficient quantity of check wells drilled before the shaft construction;

2. Heterogeneity and anisotropy of the real rock mass.

The additional factors leading to inaccuracy in the mathematical model and also requiring adjustment of the model parameters are the following process factors:

3. The presence of voids between the rock mass and walls of the freezing wells due to poor quality cementing of well annular space;

4. Deviation of well axes positions from the vertical due to the imperfection of well drilling procedure and inaccuracy in the measurement of this deviation (well survey inaccuracy).

The third factor worsens the intensity of heat transfer, while the fourth factor leads to an inaccuracy in localizing heat sources for each rock layer. Consideration of the process factors 2–4 indicates that thermophysical properties of the medium, which are required to be determined during adjustment, will not be true thermophysical properties of this medium, but will have some effective values.

The number of parameters, which can be used to adjust a mathematical model, is determined according to the type of mathematical model, i.e. the number of independent dimensionless complexes on which the resulting solution depends—temperature distribution and concentration of the frozen phase.

To select the adjustment parameters, let us formulate a mathematical model of heat exchange processes occurring in a water-saturated horizontal layer of the rock mass with isotropic and homogeneous properties during its artificial freezing (Fig. 3). It is assumed that the heat transfer in the vertical direction is negligible compared to the horizontal direction [7], which makes it possible to proceed to a two-dimensional formulation. The moisture migration under the action of pressure and temperature gradients is not taken into consideration. It is also assumed that the phase transition takes place in a preset temperature range according to a linear law [12, 13], which is expressed by the following functional dependence of specific enthalpy H on temperature T:

$$H(T) = \begin{cases} \rho_{th} c_{th} (T - T_{p2}) + \rho_{th} w L, & T_{p2} < T, \\ \rho_{th} w L \phi_{ice}, & T_{p1} < T < T_{p2}, \\ \rho_{fr} c_{fr} (T - T_{p1}), & T < T_{p1}. \end{cases} \tag{3}$$

Here, ρ is the density, kg/m^3; c is the specific heat of soil per unit mass, J/(°C·kg); w is the moisture content in soil, kg/kg; L is the specific heat of phase transition, J/kg; T_{p1} and T_{p2} are the temperatures of the beginning and end of crystallization, °C; ϕ_{ice} is the solid phase concentration of groundwaters. The index "*th*" corresponds to thawed rocks, "*fr*"—to frozen rocks.

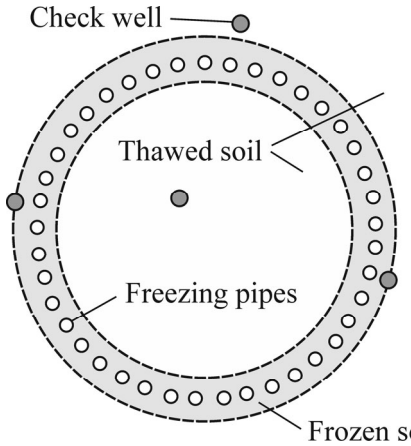

Fig. 3. Horizontal layer of the rock mass, loop of freezing pipes, check wells.

It is assumed that ice concentration in porous rock mass increases linearly with decreasing temperature, since this is in good agreement with laboratory tests for samples of the rocks in question. In some cases, the ice concentration may increase according to a more pronounced nonlinear law [14].

In accordance with (3), the formulation of mathematical model is made in enthalpy form [3, 15–17]:

$$\frac{\partial H}{\partial t} = \frac{\partial}{\partial x}\left[\lambda(T)\frac{\partial T}{\partial x}\right] + \frac{\partial}{\partial y}\left[\lambda(T)\frac{\partial T}{\partial y}\right], \tag{4}$$

$$\left[\lambda(T)\frac{\partial T}{\partial n} - \alpha(T_F - T)\right]\Big|_{\Omega_F} = 0, \tag{5}$$

$$T\big|_{\Omega_{out}} = T_0, \tag{6}$$

$$T\big|_{t=0} = T_0, \tag{7}$$

$$\phi_{ice}(H) = \begin{cases} 1, & H < 0, \\ \dfrac{H}{\rho_{th} wL}, & 0 < H < \rho_{th} wL, \\ 0, & \rho_{th} wL < H, \end{cases} \tag{8}$$

where $\lambda(\phi_{ice}) = \phi_{ice}\lambda_{fr} + (1-\phi_{ice})\lambda_{th}$ is thermal conductivity function of the rock mass from ice phase concentration, W/(°C·m); t is physical time, c; α is the heat transfer coefficient, W/(°C·m^2); T_0 is the temperature of undisturbed rock mass, C; T_F is the brine temperature in freezing pipes, C; (x, y) are the physical coordinates, m; $\Omega_F = \bigcup\Omega_{Fi}$ are the boundaries with all freezing pipes $i = 1,..., N$; Ω_{out} is the outer boundary of modeling domain; n is the coordinate along the normal to Ω_F, m.

To write the system of equations (3)–(8) in the dimensionless form, the respective variables are introduced:

$$X = \frac{x}{l}, \quad Y = \frac{y}{l}, \quad N = \frac{n}{l}, \quad \tau = \frac{t}{t_\Sigma}, \quad \Theta = \frac{T - T_0}{T_F - T_0}, \quad \mathrm{H} = \frac{H}{\rho_{th} wL}. \tag{9}$$

The index i takes the value "*th*" or "*fr*"; t_Σ is total modeling time, s; l is characteristic length (the radius of design contour of freezing pipes can serve as this value), m.

Two-dimensional two-phase Stefan problem (3)–(8) in dimensionless coordinates for the horizontal layer of rocks has the following form:

$$\frac{\partial \mathrm{H}(\Theta)}{\partial \tau} = \mathrm{Fo}_{th}\mathrm{Ste}_{th}\left\{\frac{\partial}{\partial X}\left[1 + \phi_{ice}\left(\frac{\lambda_{fr}}{\lambda_{th}} - 1\right)\right]\frac{\partial \Theta}{\partial X} + \frac{\partial}{\partial Y}\left[1 + \phi_{ice}\left(\frac{\lambda_{fr}}{\lambda_{th}} - 1\right)\right]\frac{\partial \Theta}{\partial Y}\right\}, \tag{10}$$

$$\left[\frac{\partial \Theta}{\partial N} - \mathrm{Bi}(\Theta_F - \Theta)\right]\Big|_{\Omega_F} = 0, \tag{11}$$

$$\Theta\big|_{\Omega_{out}} = 0, \tag{12}$$

$$\Theta\big|_{\tau=0} = 0, \tag{13}$$

$$\mathrm{H}(\Theta)=\begin{cases}\mathrm{Ste}_{th}(\Theta-\Theta_{p2})+1, & \Theta_{p2}<\Theta,\\ \phi_{ice}, & \Theta_{p1}<\Theta<\Theta_{p2},\\ \dfrac{\mathrm{Ste}_{fr}(\Theta-\Theta_{p1})\rho_{fr}}{\rho_{th}}, & \Theta<\Theta_{p1},\end{cases} \tag{14}$$

$$\phi_{ice}(\mathrm{H})=\begin{cases}1, & \mathrm{H}<0,\\ \mathrm{H}, & 0<\mathrm{H}<1,\\ 0, & 1<\mathrm{H},\end{cases} \tag{15}$$

where τ is the dimensionless time variable; X, Y are the dimensionless coordinates; $\Theta_F=1$ is the dimensionless freezing temperature; $\Theta_0=0$ is the dimensionless temperature of undisturbed rock mass; $\Omega_F=\bigcup\Omega_{Fi}$ are the boundaries with all freezing pipes $i=1,...,N$; Ω_{out} is the outer boundary of modeling domain; N is dimensionless coordinate along the normal to Ω_F; $\mathrm{Bi}=\alpha l/\lambda_{fr}$ is the dimensionless Biot number.

The system of equations (10)–(15) allows finding the distribution of temperatures Θ as a function of two dimensionless coordinates X and Y, two dimensionless temperatures of phase transition Θ_{p1}, Θ_{p2} and six dimensionless complexes Fo_{th}, Ste_{th}, Ste_{fr}, Bi, ρ_{fr}/ρ_{th}, $\lambda_{fr}/\lambda_{th}$. Under high hydrostatic stress of rocks at a depth, the rock density changes insignificantly, and the complex ρ_{fr}/ρ_{th} can be excluded from consideration.

Since moisture migration is absent in this model, the moisture content of water-saturated rock mass in the solid and liquid phases will be the same. In this case, instead of the criterion $\lambda_{fr}/\lambda_{th}$, we can take Fo_{fr} expressed in terms of other criteria:

$$\frac{\mathrm{Fo}_{fr}}{\mathrm{Fo}_{th}}\frac{\mathrm{Ste}_{fr}}{\mathrm{Ste}_{th}}=\frac{\dfrac{\lambda_{fr}t_\Sigma}{\rho c_{fr}l^2}}{\dfrac{\lambda_{th}t_\Sigma}{\rho c_{th}l^2}}\frac{\dfrac{c_{fr}(T_F-T_0)}{wL}}{\dfrac{c_{th}(T_F-T_0)}{wL}}=\frac{\lambda_{fr}}{\lambda_{th}}. \tag{16}$$

This expression is written under the condition of equal rock mass density in thawed and frozen states.

Taking into account the accepted simplifications, the solution of problem (10)–(15) depends on 5 dimensionless complexes, which contain the information about thermophysical properties of the medium under consideration: Fo_{th}, Fo_{fr}, Ste_{th}, Ste_{fr}, Bi, and two dimensionless temperatures Θ_{p1}, Θ_{p2} characterizing phase transition.

In the simplest case, up to 5 thermophysical properties included into dimensionless complexes presented above can be taken as adjustment parameters of the heat transfer model in the "rock mass–freezing wells" system. In a more complex case, the condition of minimum integral deviation of ajustable thermophysical parameters p_i from their initial values $p_i^{(0)}$ obtained from engineering and geological surveys can be additionally considered. For example, the following functional can be chosen:

$$F=\sqrt{\sum_i (p_i-p_i^{(0)})^2}\to\min. \tag{17}$$

In this case, a greater number of adjustment parameters can be selected.

In this study, the conditions for minimum integral deviation of adjustable thermophysical parameters from their initial values will not be considered. It is also assumed that the temperatures of the beginning and end of the phase transition Θ_{p1} and Θ_{p2} are unalterable.

2. FORMULATION OF THE OF INVERSE STEFAN PROBLEM

The purpose of the analysis of direct Stefan problem in dimensionless quantities was to determine the number of dimensionless complexes on which the solution—the temperature field depends. This objective has been accomplished, so for convenience we will make the transition back to the system of dimensional values.

Adjustment of the thermophysical parameters from problem (3)–(8) represents the solution to coefficient inverse Stefan problem [18, 19]. To formulate the inverse problem, let us redefine the direct problem (3)–(8) by introducing preset measured temperatures $T_i^{(c)}(t)$ to the location place (x_t, y_i) of each check well no. i:

$$T(t, x, y) = T_i^{(c)}(t), \quad i = 1,..., N_C, \tag{18}$$

N_C is the number of check wells.

The solution to inverse Stefan problem is to determine the temperature field $T(t, x, y)$ and the values of thermophysical parameters of the rock mass satisfying the system of equations (3)–(8), (18). Instead of stringent condition (18), the functional of discrepancies between the theoretical and experimentally measured temperatures in the check wells was considered in this paper: (2). The solution to the inverse Stefan problem consists in minimization of functional (2) subject to conditions (3)–(8) [18, 20].

3. STUDY OF TEMPERATURE DISCREPANCY FUNCTIONAL

The type of functional I in the phase space of rock mass thermophysical properties was investigated. A multiparameter numerical calculation of direct two-dimensional Stefan problem for horizontal layer of rocks was carried out. The finite difference method, an explicit scheme for the enthalpy formulation of the Stefan problem on a regular inhomogeneous Cartesian grid with condensations near freezing wells was applied (Fig. 4). The choice in favor of the Cartesian grid in this case is due to the fact that with increasing depth, the freezing pipes are significantly shifted relative to the initial ideal circular contour, as a result of which the advantage, for example, of polar grid disappears.

The grid size at a distance from the wells and condensation near the wells were selected on the basis of preliminary calculations in such a way as to ensure temperature distribution that does not depend on the grid properties. At the boundary with freezing wells, the heat flow was calculated from the effective heat exchange area, formed by the faces of the cells bordering the wells (Fig. 5). When calculating the value of heat flow through the effective area, a reduction factor, equal to the physical/effective heat exchange area ratio, was used.

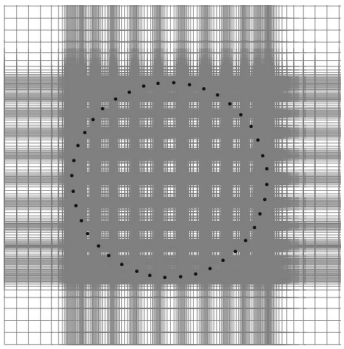

Fig. 4. Finite-difference grid.

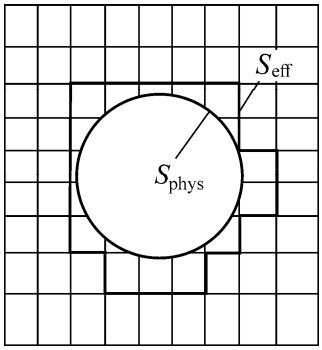

Fig. 5. Physical S_{phys} and effective S_{eff} surfaces of heat exchange of freezing wells.

The number of cells in the final grid adopted for calculations was 172040. The grid quality was estimated according to the Maximum aspect ratio criterion, which is equal for the case of a regular grid to the maximum ratio of two characteristic cell sides. The value of the criterion for all grid cells is not more than 20, which is admissible. In the numerical solution of system (3)–(8), an explicit first-order in time and second-order in space schemes were used. To speed up the calculations, parallelizing was performed on the CPU cores using the TPL.Net Framework library.

As a result of multiparameter numerical calculation of direct Stefan problem, the dependences of temperature discrepancy functional on thermophysical properties—thermal conductivities and heat capacities of the frozen and thawed rock mass, and moisture content were obtained (Fig. 6). The calculation was carried out for the following set of parameters: freezing wells radius—0.073 m; the number of freezing wells—41; the radius of circular contour of freezing wells—8.5 m; width and height of the computational domain—30 m; rock mass density in thawed and frozen state—2000 kg/m^3; moisture content in the rock mass in the thawed and frozen state—0.2 kg/kg; brine temperature in freezing wells— –20°C; brine consumption in freezing wells—10 m^3/h; the temperature of undisturbed rock mass— +10°C; chilling temperature of groundwater—0°C; temperature of complete crystallization of groundwater— –1°C; the number of check wells—1.

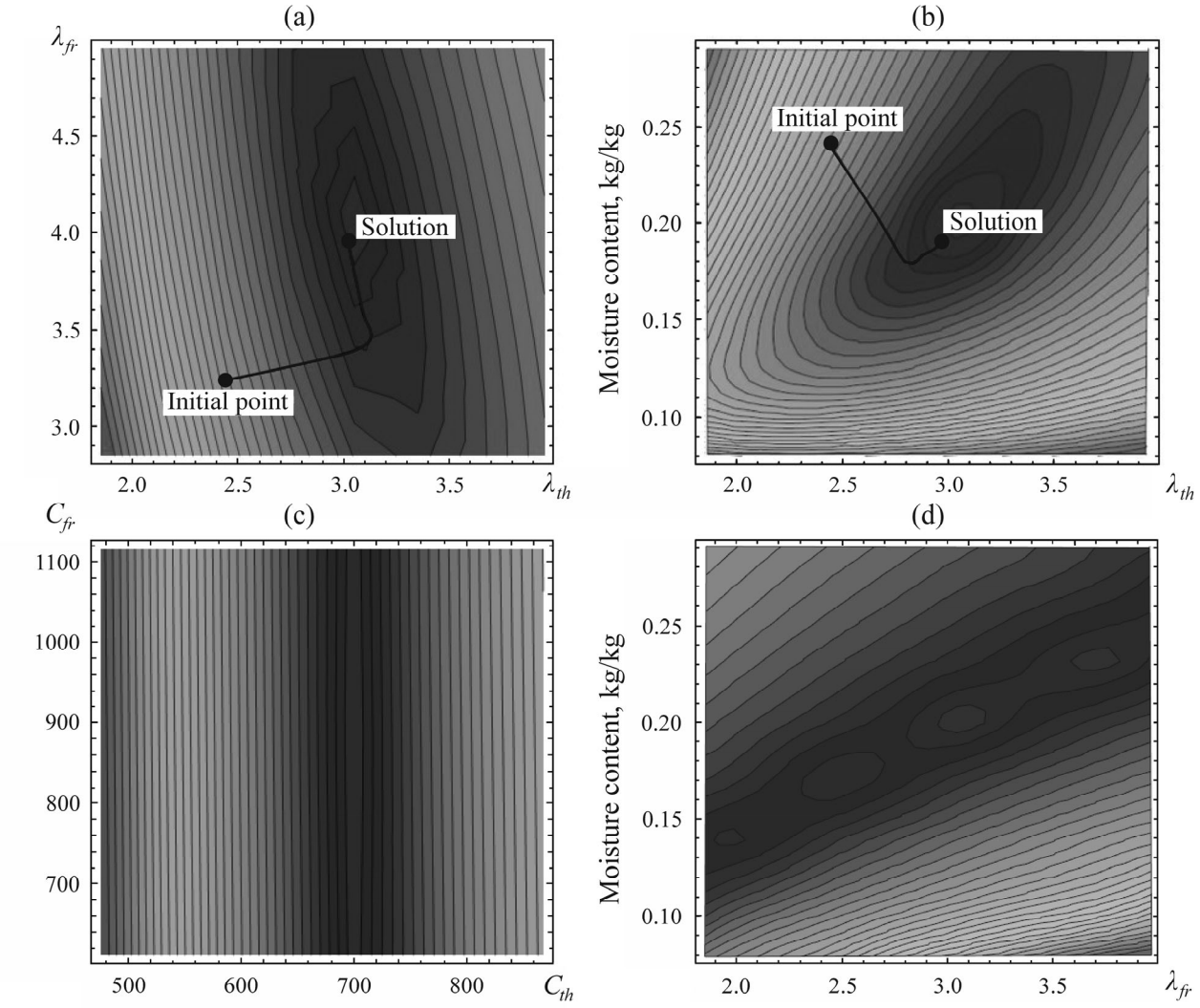

Fig. 6. Temperature discrepancy functional of rocks in check thermal wells: (a) as a function of thermal conductivity of the thawed and frozen rock mass; (b) as a function of thermal conductivity of the thawed rock mass and moisture content; (c) as a function of heat capacities of the thawed and frozen rock mass; (d) as a function of moisture content and thermal conductivity of the frozen rock mass.

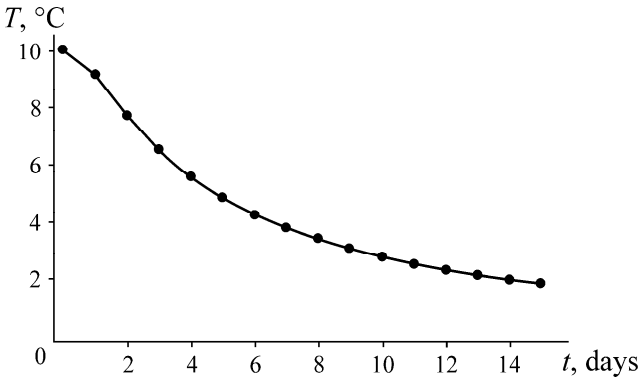

Fig. 7. Time dependence of rock mass temperature in model check well.

The function $T_c(t)$ obtained as a result of solution to direct Stefan problem was accepted as the temperature measured in check well, for parameters: heat capacity of the thawed soil—900 J/(kg·°C); heat capacity of the frozen soil—700 J/(kg·°C); thermal conductivity of the thawed soil—3 W/(m·°C); thermal conductivity of the frozen soil—4 W/(m·°C) (Fig. 7).

The temperature discrepancy functional has a pronounced minimum on the phase plane of variation in soil thermal conductivities (Fig. 6a). With increasing time, the isolines of discrepancy functional on the plane of soil thermal conductivities tend from an elongated ellipsoidal shape to a circular one, which is caused by an increase of the frozen soil zone and increased effect of thermal conductivity of the frozen soil on the temperature field [21]. At short modeling times, when the ice zone occupies a relatively small part of the computational domain, the effect of thermal conductivity of frozen soil is manifested in the boundary condition at the wells, determined by the Biot number, and at the phase transition front in $\mathrm{Fo}_{fr}\mathrm{Ste}_{fr}$ complex. In the range of parameters under study (Fig. 6), a small modeling time is a time in the range from 0 to 30 days.

The temperature discrepancy functional is almost independent of the heat capacity of frozen rock mass for the case under consideration, due to the fact that at short modeling times the temperature distribution in the ice zone is established much faster, than the phase transition boundary moves (Fig. 6c). Hence, thermal conductivity of the frozen soil as an inertia measure of heat distribution in it does not play a significant role in this range of values.

At small modeling times, ambiguity is also observed in determination of moisture content and thermal conductivity of frozen rock mass (Fig. 6d). When considering the moisture content and thermal conductivity of thawed rock mass, such ambiguity was not revealed and the functional (1) had a clear minimum (Fig. 6b). This is stipulated by the fact that at small modeling times, the solution depends on the complex $\mathrm{Fo}_{fr}\mathrm{Ste}_{fr}$ (heat flow to the frozen soil), in which moisture content and thermal conductivity of frozen rock mass are present only in the form of relationship.

4. SOLUTION ALGORITHM FOR THE INVERSE STEFAN PROBLEM

Minimization of the functional (2) in the phase space of thermophysical properties of the rock mass was carried out using a modification of the gradient descent method. At each iteration of $N+1$ time algorithm, a direct Stefan problem is solved to determine partial derivatives of the functional F using N different minimization parameters.

Let $\mathbf{p} = (p_1, ..., p_n)$ be the vector of adjustable problem parameters; I is the current value of discrepancy functional also representing the error of inverse problem calculation; $\varepsilon_{\max}$ is the maximum admissible error of inverse problem solution. Then the algorithm proposed includes the following steps:

1. Determination of the initial approximations of $\mathbf{p}^0$.

2. Calculation of direct Stefan problem, determination of the current error I by the formula (2), comparison with the maximum admissible error $\varepsilon_{\max}$. If $I < \varepsilon_{\max}$, then the required accuracy is obtained and calculation should be completed, otherwise return to step 3.

3. Selection of small deviations of the adjustable parameters $\Delta\mathbf{p}^k$ at -kth iteration of the algorithm. Calculation of direct Stefan problem for each component of the vector $\Delta\mathbf{p}^k$. Calculation of partial derivatives of the functional I:

$$\frac{\Delta I^k}{\Delta p_i} = \frac{I(p_i^k + \Delta p_i) - I(p_i^k)}{\Delta p_i}, \quad \nabla I^k = \left(\frac{\Delta I^k}{\Delta p_1}, ..., \frac{\Delta I^k}{\Delta p_n} \right). \tag{19}$$

4. Calculation of the new values of adjustable parameters at $(k+1)$th iteration of the problem using the formula:

$$\Delta\mathbf{p}^k = \mu\Delta\mathbf{p}^{k-1} + (1-\mu) I^k \frac{\nabla I^k}{\left|\nabla I^k\right|}, \quad \mathbf{p}^{k+1} = \mathbf{p}^k + \sigma\Delta\mathbf{p}^k, \tag{20}$$

where $\mu \in [0, 1)$ is the parameter characterizing the past history factor; $\sigma > 0$ is the parameter determining the velocity of gradient descent.

5. Check for the entry of adjustment parameters into the range of admissible values:

$$p_i^k \in [p_{i\,\min}, p_{i\,\max}], \quad i = 1, ..., N_C. \tag{21}$$

6. If the maximum number of iterations is exceeded, then calculation should be completed, otherwise return to step 2.

Figures 6a, b present the solution to inverse Stefan problem using this algorithm for the parameters $\mu = 0.4$ and $\sigma = 1$.

The solution algorithm to inverse Stefan problem is implemented in the C# language in Visual Studio medium and included as the basic axial module into Frozen Wall software system developed by Mining Institute of the Ural Branch of the Russian Academy of Sciences.

CONCLUSIONS

The two-dimensional two-phase direct Stefan problem in dimensionless coordinates has been formulated. Based on the fact that there are 5 different dimensionless complexes characterizing thermophysical properties of the rock mass in this problem, it was concluded that in the proposed statement of the problem, no more than 5 different independent thermophysical properties should be adjusted. Adjustment of “water-ice” phase transition parameters was not considered in this paper.

The formulation of the inverse Stefan problem consisted in minimizing the discrepancy functional of the numerically calculated and experimentally measured temperatures in check wells. The discrepancy functional properties have been investigated. It was obtained that at the

initial stage of frozen wall forming at small times (up to 30 days), heat capacity of the frozen soil should not be adjusted, moisture saturation and thermal conductivity of the frozen soil should not be adjusted simultaneously.

An iteration algorithm for solving the inverse Stefan problem has been formulated. The presented algorithm as a part of FrozenWall software system was used to adjust thermophysical parameters of the rock mass layers when sinking shafts of the Nezhinsky GOK mine by artificial freezing. As a result of mathematical prediction of frozen wall condition using the adjusted properties, a time period was determined during which a frozen wall of preset thickness was formed, after which recommendations were given on the beginning of sinking mine shafts nos. 1–2.

FUNDING

This work was supported by the Russian Science Foundation, project no. 17-11-01204.

REFERENCES

1. Trupak, N.G, *Zamorazhivanie gornykh porod pri prokhodke stvolov* (Freezing of Rocks in Shaft Sinking), Moscow: Ugletekhizdat, 1954.
2. Safety Rules in Underground Structures Construction PB 03-428-02. Approved by Gosgortekhnadzor of Russia on 02.11.2001, No. 49.
3. Levin, L.Yu., Semin, M.A., and Zaitsev, A.V., *Kontrol i prognoz formirovaniya ledoporodnogo ograzhdeniya s ispolzovaniem optovolokonnykh tekhnologiy. Strategiya i protsessy osvoeniya georesursov: sb. nauch. tr.* (Control and Prediction of Frozen Wall Formation Using Optic Fiber Technologies. Strategy and Processes of Georesources Development: Collected Papers), Perm: GI UrO RAN, 2016.
4. Amosov, P.V., Lukichev, S.V., and Nagovitsyn, O.V., Influence of Rock Mass Porosity and Cooling Agent Temperature on Frozen Wall Formation Rate, *Vestn. KNTS RAN*, 2016, vol. 27, no. 4, pp. 43–50.
5. Gendler, S.G., Integrated Safety Provision in Developing Mineral and Spatial Subsol Resources, *Gornyi Zhurnal*, 2014, no. 5, pp. 5–6.
6. Sopko, J., Coupled Heat Transfer and Groundwater Flow Models for Ground Freezing Design and Analysis in Construction, *Geotech. Frontiers*, 2017, p. 11.
7. Vitel, M., Rouabhi, A., Tijani, M., and Guerin, F., Modeling Heat Transfer between a Freeze Pipe and the Surrounding Ground during Artificial Ground Freezing Activities, *Comput. Geotech.*, 2015, vol. 63, pp. 99–111.
8. Kim, Y.S., Kang, J.M., Lee, J., Hong, S., and Kim, K.J., Finite Element Modeling and Analysis for Artificial Ground Freezing in Egress Shafts, *J. Civ. Eng.*, 2012, vol. 16, no. 6, pp. 925–932.
9. Schmall, P.C. and Maishman, D., Ground Freezing a Proven Technology in Mine Shaft Sinking, *Tunnels and Underground Construction Magazine*, 2007, vol. 59, no. 6, pp. 25–30.
10. Igolka, D.A., Igolka, E.Yu., Luksha, E.M., and Kologrivenko, A.A., Frozen Wall Temperature Effect in Designing Casing for Mine Shafts, *Gorn. Mekh. Mashinostr.*, 2014, no. 3, pp. 36–41.
11. Levin, L.Yu., Semin, M.A., Parhsakov, O.S., and Kolesov, E.V., A Method for Inverse Stefan Problem Solution to Monitor Frozen Wall Condition in Shaft Sinking, *Geolog. Neftegaz. Gorn. Delo*, 2017, vol. 16, no. 3, pp. 255–267.
12. Jame, Y.W., Heat and Mass Transfer in Freezing Unsaturated Soil, *Ph.D. Dissertation*, University of Saskatchewan, 1977.

13. McKenzie, J.M., Voss, C.I., and Siegel, D.I., Groundwater Flow with Energy Transport and Water-Ice Phase Change: Numerical Simulations, Benchmarks, and Application to Freezing in Peat Bogs, *Adv. Water Resour.*, 2007, vol. 30, no. 4, pp. 966–983.
14. Kurylyk, B.L. and Watanabe, K., The Mathematical Representation of Freezing and Thawing Processes in Variably-Saturated, Non-Deformable Soils, *Adv. Water Resour*., 2013, vol. 60, pp. 160–177.
15. Dmitriev, A.P. and Goncharov, S.A., *Termodinamicheskie protsessy v gornykh porodakh* (Thermodynamic Processes in Rocks), Moscow: Nedra, 1990.
16. Budak, B.M., Solov'eva, E.N., and Uspenskii, A.B., Difference Method with Coefficient Smoothing for Solving Stefan Problems, *ZHVMiMF*, 1965, vol. 5, no. 5, pp. 828–840.
17. Shamsundar, N. and Sparrow, E.M., Analysis of Multidimensional Conduction Phase Change via the Enthalpy Model, *J. Heat Transfer*, 1975, vol. 97, no. 3, pp. 333–340.
18. Alifanov, O.M., *Obratnye zadachi teploobmena* (Inverse Problems of Heat Exchange), Moscow: Mashinostroenie, 1988.
19. Tikhonov, A.N. and Arsenin, V.Y., *Solutions of Ill-Posed Problems*, Washington, DC: Winston & Sons, 1977.
20. Levin, L.Yu., Semin, M.A., Bogdan, S.I., and Zaitsev, A.V., Solution of Inverse Stefan Problem when Analyzing Groundwater Freezing in the Rock Mass, *IFZH*, 2018, vol 91, no. 3, pp. 655–663.
21. Levin, L.Yu., Semin, M.A., and Parhsakov, O.S., Mathematical Prediction of Frozen Wall Thickness in Shaft Sinking, *J. Min. Sci.*, 2017, vol. 53, no. 5, pp. 154–161.